Modeling and Simulation Technique of Two Quadrant Chopper and PWM Inverter-Fed IPMSM Drive System and Its Application to Hybrid Vehicles

Toshiaki Murata*, Utaro Kawatsu*, Junji Tamura*, and Takeshi Tsuchiya*

Abstract – This paper presents a state space model of a two quadrant chopper and PWM inverter-fed Interior Permanent Magnet Synchronous Motor (IPMSM) drive system and its application to hybrid vehicles. The drive system has two different state equations for motoring and regenerating action. This paper presents a common state equation by using State Space Averaging method. Using this model of the IPMSM drive system, detailed simulation and controller design of the drive system, including PWM inverter switching, are given. The validity of this model and usefulness, according to a comparison among Maximum Torque/Ampere control, Maximum Torque/Flux control, and Maximum Efficiency optimization, are confirmed from simulation results.

Keywords: Two quadrant chopper, PWM inverter, IPMSM Drive, Hybrid Vehicles

1. Introduction

Recently, unfavorable Earth environment due to exhaust gas from cars has become more serious and crude prices are continuing to show fantastic rises. The government is urged to take new measures against these problems. One possible solution of these problems is the development of hybrid vehicles using a PMSM [1]~[3]. It was considered that the inverter supply voltage should be higher as a means to improve the output of a motor . But, when using a battery as the supply, it is necessary to use many batteries in series to increase the voltage. That is, when the voltage is higher, more batteries are required. Also, the cost is higher than that of capacitors and batteries occupy more space.

Variable voltage system is presented to solve such a problem by using a buck-boost chopper. The inverter voltage can be varied optionally by the buck-boost chopper. Then the number of batteries decreases. In order to step up the DC link voltage, a model of a two quadrant chopper and PWM inverter-fed IPMSM drive system for hybrid vehicles is designed and presented, together with an equivalent circuit of the IPMSM, taking core losses into account. A hybrid vehicle may be operated under variable load torque conditions. Some torque control strategies, such as maximum-torque control and efficiency-optimized control, are presented. The control system designed with optimal regulator theory is operated by an algorithm utilizing Maximum Torque/Ampere control. The usefulness of its application to the hybrid vehicle is confirmed by using a reduced IPMSM model to simulate a laboratory machine and by driving the IPMSM with the quadrant chopper and PWM inverter to regenerate the power by switching to the buck-boost chopper. The validity of the model is confirmed from simulation results.

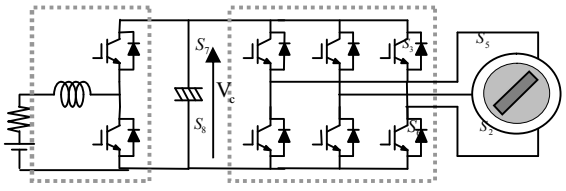

Fig. 1. Modeling of IPMSM drive system

2. Modeling of The Drive System

The two-quadrant chopper and PWM inverter-fed IPMSM drive system is shown in Fig.1. In Fig.1, the resistance R and inductance L are the internal resistance and inductance of the battery, respectively. Fig.2 shows equivalent circuits of the motoring and regenerating modes of the two-quadrant chopper. The following equations are obtained from Fig.2.

* Dept. of Electrical Engineering, Kitami Institute of Technology, Japan. Hokkaido Institute of Technology, Japan(ICJ33288@nifty.com)
Received 13 July 2011 ; Accepted 14 August 2011

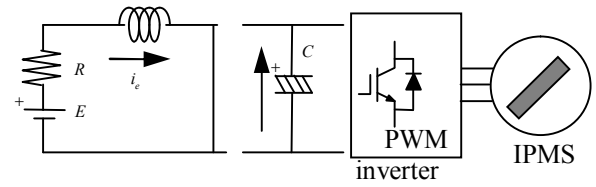

(a) Equivalent circuit (S_7 off, S_8 on) for motoring action

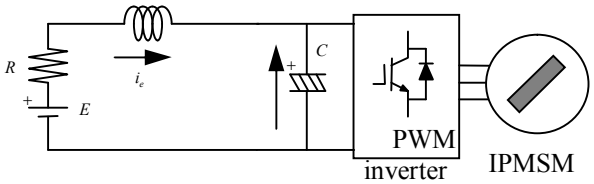

(b) Equivalent circuit (S_7 on, S_8 off)

Fig. 2. Modeling of Two quadrant chopper

Under motoring action in Fig.2(a),

$$0 = -CV_C \frac{dV_C}{dt} + v_d i_d + v_q i_q \tag{1}$$

$$Ei_e = Ri_e^{\,2} + Li_e \frac{di_e}{dt} - CV_C \frac{dV_C}{dt} + v_d i_d + v_q i_q \tag{2}$$

Under regenerating action in Fig.2(b),

$$v_d i_d + v_q i_q = CV_C \frac{dV_C}{dt} \tag{3}$$

$$v_d i_d + v_q i_q = CV_C \frac{dV_C}{dt} + Li_e \frac{di_e}{dt} + Ri_e^{\,2} + Ei_e \tag{4}$$

There are two different state equations for the motoring action and regenerating action by switching. The two-quadrant chopper is modeled by considering the State Space Averaging Method [4], in which the state equation for the "on" state (S_7 off, S_8 on in Fig.1) is multiplied by a duty factor α, and the state equation for the "off" state (S_7 on, S_8 off in Fig.1) is multiplied by a duty factor (1- α), in order to get the average from the control input α. The following equations are expressed by using the State Space Averaging method.

$$\frac{di_e}{dt} = -\frac{R}{L} i_e - \frac{1-\alpha}{L} V_C + \frac{1}{L} E \tag{5}$$

$$\frac{dV_C}{dt} = \frac{1-\alpha}{C} i_e - \frac{3}{2} \frac{1}{CV_C \left(R_a + R_m\right)} (v_d^{\,2} + R_m v_d i_{md} + v_q^{\,2} + R_m v_q i_{mq}) \tag{6}$$

State equations for the IPMSM, considering core losses, are shown in the appendix. State equations of the drive system, considering the mechanical torque equation, are presented as follows.

$$\frac{d\omega_{me}}{dt} = -\frac{D}{J}\omega_{me} + \frac{p^2}{J}\left\{\left(L_d - L_q\right) i_{md} i_{mq} + \phi_a i_{mq}\right\} - \frac{p}{J}\tau_l \tag{7}$$

$$\frac{di_{md}}{dt} = \omega_{me} i_{mq} \frac{L_q}{L_d} - \left(\frac{R_m}{R_a + R_m}\right)\frac{R_a}{L_d} i_{md} + \left(\frac{R_m}{R_a + R_m}\right)\frac{v_d}{L_d} \tag{8}$$

$$\frac{di_{mq}}{dt} = -\frac{\omega_{me}}{L_q}\left(L_d i_{md} + \phi_a\right) - \left(\frac{R_m}{R_a + R_m}\right)\frac{R_a}{L_q} i_{mq} \tag{9}$$

$$\frac{di_e}{dt} = -\frac{R}{L} i_e - \frac{1-\alpha}{L} V_C + \frac{1}{L} E \tag{10}$$

$$\frac{dV_C}{dt} = \frac{1-\alpha}{C} i_e - \frac{3}{2} \frac{1}{CV_C \left(R_a + R_m\right)} (v_d^{\,2} + R_m v_d i_{md} + v_q^{\,2} + R_m v_q i_{mq}) \tag{11}$$

Control inputs of the state space model of the IPMSM drive system are the d-q axes voltages v_d, v_q and duty factor α.

3. Control Strategy

It is necessary to control both the amplitude and phase of the armature current of the IPMSM for torque control. Recent control strategies of the IPMSM are Maximum Torque/Ampere control (MTPA control) [5], Maximum Torque/Flux control (MTPF control), and Maximum Efficiency control (ME control) [6] as follows.

3.1 Maximum Torque / Ampere (MTPA) Control

A condition producing maximum torque and minimum magnetizing current exists. In this condition, the copper loss becomes minimum, because the magnetizing current is minimum. In order to simplify the torque equation (see eq.(A-6)), the torque equation is expressed using the following relations.

$$i_{mq} = \sqrt{i_m^{\,2} - i_{md}^{\,2}}, \quad i_m = \sqrt{i_{md}^{\,2} + i_{mq}^{\,2}} \tag{12}$$

The torque equation in eq.(A-6) can be expressed ~~by~~ in terms of the magnetizing currents i_{md} and i_m. Setting $\partial T_e / \partial i_{md} = 0$, the following desired current $i_{md}^{\,R}$ is obtained.

$$i_{md}^{\,R} = \frac{-\phi_a + \sqrt{\phi_a^{\,2} + 8\left(L_d - L_q\right)^2 i_m^{\,2}}}{4\left(L_d - L_q\right)} \tag{13}$$

Then, the error e_i can be defined as

$$e_i = i_{md}^{\,R} - i_{md} \tag{14}$$

The error e_i can be controlled to be zero by using the Maximum Torque/Ampere control method.

3.2 Maximum Torque /Flux (MTPF) Control

In order to simplify the torque equation, the torque is expressed using the following relations.

$$i_{mq}=\frac{\sqrt{\lambda^2-\lambda_d{}^2}}{L_q}=\frac{\sqrt{\lambda^2-\left(L_d i_{md}+\phi_a\right)^2}}{L_q},\lambda=\sqrt{\lambda_d{}^2+\lambda_q{}^2} \quad (15)$$

The condition minimizing the linkage flux for a given developed torque exists. Rewriting eq.(A-6),

$$T_e=p\{(L_d-L_q)i_{md}+\phi_a\}\frac{\sqrt{\lambda-(L_d i_{md}+\phi_a)^2}}{L_q} \quad (16)$$

Setting $\partial T_e/\partial i_{md}=0$, the following desired current $i_{md}{}^R$ is obtained, similar to the case of the MTPA control.

$$i_{md}{}^R=\frac{-4\phi_a\left(L_d-L_q\right)+L_q\phi_a-\sqrt{L_q{}^2\phi_a{}^2+8\left(L_d-L_q\right)^2\lambda^2}}{4L_d\left(L_d-L_q\right)} \quad (17)$$

3.3 Maximum Efficiency Optimization (ME) Control

A controllable loss, P_{loss}, defined from copper loss and iron loss in terms of the magnetizing current components, can be written as follows:

$$\begin{aligned}P_{loss}&=R_a i_a{}^2+R_m i_c{}^2\\&=K_1 i_{md}{}^2+K_2 i_{mq}{}^2+K_3 i_{md}i_{mq}+K_4 i_{md}+K_5 i_{mq}+K_6\end{aligned} \quad (18)$$

where

$$K_1=R_m L_d{}^2+R_a,\quad K_2=R_m L_d{}^2+R_a$$
$$K_3=2\omega_{me}R_a\left(L_d-L_q\right)/R_m,\quad K_4=2R_m\phi_a L_d$$

The q-axis magnetizing current can be written in terms of the torque as follows.

$$\begin{aligned}i_{mq}&=T_e/\left(K_7+K_8 i_{md}\right)\\K_7&=p\phi_a,\quad K_8=p\left(L_d-L_q\right)\end{aligned} \quad (19)$$

Substituting eq. (19) into eq. (18), differentiating the controllable loss with respect to i_{md}, and setting this differentiation to zero, the following relation is obtained:

$$K_{11}i_{md}{}^4+K_{12}i_{md}{}^3+K_{13}i_{md}{}^2+K_{14}i_{md}+K_{15}=0 \quad (20)$$

where

$$K_{11}=2K_1K_8{}^3,\quad K_{12}=\left(6K_1K_7+K_4K_8\right)K_8{}^2$$
$$K_{13}=3\left(2K_1K_7+K_4K_8\right)K_7K_8$$
$$K_{14}=\left(2K_1K_7+3K_4K_8\right)K_7{}^2+\left(K_3K_7-K_5K_8\right)T_eK_8$$
$$K_{15}=\left(K_4K_7+K_3T_e\right)K_7{}^2-\left(2K_2T_m+K_5K_7\right)K_8T_e$$

It is seen from eq. (20) that there is a value of i_{md} at which the controllable loss is minimum and the efficiency is maximum. This value of i_{md} can be defined as the optimal d-axis magnetizing current $\tilde{i}_{md}$. Fig.3 shows a comparison of the efficiency of the MTPF, MTPA, and ME control methods. Maximum efficiency operation is expected over a wide range, as seen from Fig.3.Higher efficiency is obtained by MTPF control, more than that by MTPA control, in the high speed range. The control strategy should be selected according to the application.

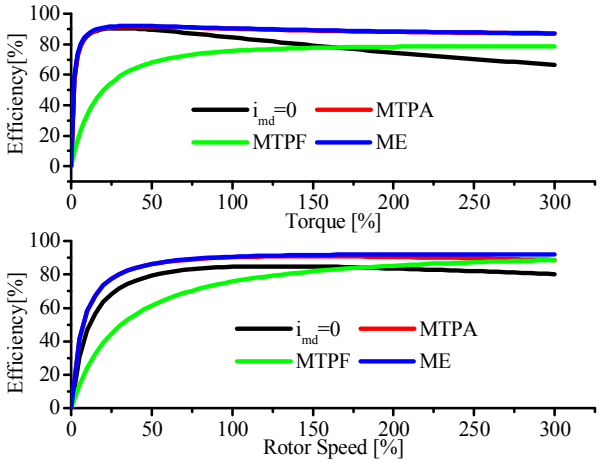

Fig. 3. Efficiency of control methods

4. Control System Structure

After linearization of the state equations and output equation of the IPMSM drive system at steady state operation , the discrete time forms are presented as follows.

$$\mathbf{x}(\mathrm{k}+1)=\mathbf{A}\mathbf{x}(\mathrm{k})+\mathbf{B}\mathbf{u}(\mathrm{k}),\ \mathbf{y}(\mathrm{k})=\mathbf{C}\mathbf{x}(\mathrm{k}) \quad (21)$$

$$\begin{aligned}&\mathbf{x}(k)=\left[\omega_{me}\quad i_{md}\quad i_{mq}\quad i_e\quad V_c\right]^T,\mathbf{y}(k)=\left[\omega_{me}\quad V_c\right]^T\\&\mathbf{u}(k)=\left[v_d\quad v_q\quad \alpha\right]^T\end{aligned} \quad (22)$$

The desired values are defined as follows.

$$\mathbf{R}(k)=\left[\omega_{me}{}^R\quad V_C{}^R\right]^T \quad (23)$$

The error for speed control is defined with the following equation:

$$\mathbf{e}(\mathrm{k})=\mathbf{R}(\mathrm{k})-\mathbf{y}(\mathrm{k}) \quad (24)$$

The error at time k+1 is defined as follows.

$$\begin{aligned}\Delta\mathbf{e}(k+1)&=\Delta\mathbf{R}(k+1)-\mathbf{C}\Delta\mathbf{x}(k+1)\\&=\Delta\mathbf{R}(k+1)-\mathbf{CA}\Delta\mathbf{x}(k)-\mathbf{CB}\Delta\mathbf{u}(k)-\mathbf{CE}\Delta\mathbf{d}(k)\end{aligned} \quad (25)$$

where the Δ operator is defined as follows.

$$\Delta\mathbf{e}(k+1)=\mathbf{e}(k+1)-\mathbf{e}(k) \quad (26)$$

The error for efficiency optimization is given as

$$e_\eta(k) = \tilde{K} i_{md}(k) - i_{mq}(k) = \begin{bmatrix} 0 & \tilde{K} & -1 & 0 \end{bmatrix} \mathbf{x}(k) = \mathbf{K}\mathbf{x}(k) \quad (27)$$

$$\tilde{K} = \tilde{i}_{md}(k) / \tilde{i}_{md}(k) \quad (28)$$

An augmented system, called error system which selects new state variables as the errors, is defined as follows:

$$\begin{bmatrix} \mathbf{e}(k+1) \\ e_\eta(k+1) \\ \Delta\mathbf{x}(k+1) \end{bmatrix} = \begin{bmatrix} \mathbf{I_m} & \mathbf{-CA} \\ \mathbf{0} & \mathbf{KA} \\ \mathbf{0} & \mathbf{A} \end{bmatrix} \begin{bmatrix} \mathbf{e}(k) \\ e_\eta(k) \\ \Delta\mathbf{x}(k) \end{bmatrix} + \begin{bmatrix} \mathbf{-CB} \\ \mathbf{KB} \\ \mathbf{B} \end{bmatrix} \Delta\mathbf{u}(k)$$

$$\begin{bmatrix} \mathbf{e}(k+1) \\ e_\eta(k+1) \\ \Delta\mathbf{x}(k+1) \end{bmatrix} = \begin{bmatrix} \mathbf{I_m} & \mathbf{-CA} \\ \mathbf{0} & \mathbf{KA} \\ \mathbf{0} & \mathbf{A} \end{bmatrix} \begin{bmatrix} \mathbf{e}(k) \\ e_\eta(k) \\ \Delta\mathbf{x}(k) \end{bmatrix} + \begin{bmatrix} \mathbf{-CB} \\ \mathbf{KB} \\ \mathbf{B} \end{bmatrix} \Delta\mathbf{u}(k) + \begin{bmatrix} \mathbf{I_m} \\ \mathbf{0} \\ \mathbf{0} \end{bmatrix} \Delta\mathbf{R}(k+1) + \begin{bmatrix} \mathbf{-CE} \\ \mathbf{KE} \\ \mathbf{E} \end{bmatrix} \Delta\mathbf{d}(k)$$

$$= \mathbf{\Psi X}_0(k) + \mathbf{G}\Delta\mathbf{u}(k) + \mathbf{G}_R\Delta\mathbf{R}(k+1) + \mathbf{G}_d\Delta d(k) \quad (29)$$

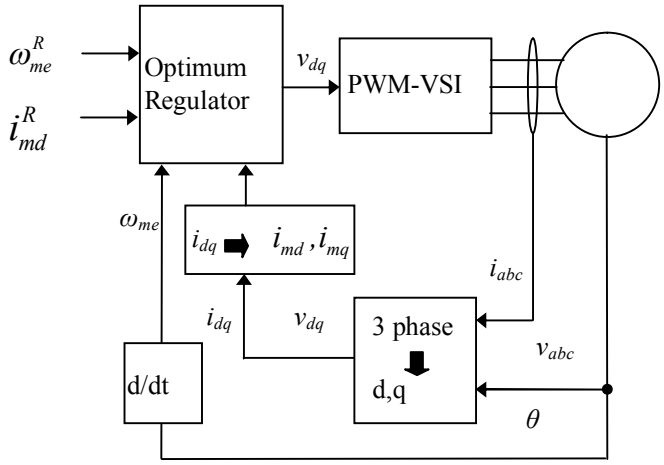

Fig. 4. Control system structure

where $\mathbf{I_m}$ is the unit matrix.

Assuming the desired value is a step change, a quadratic performance index is defined as:

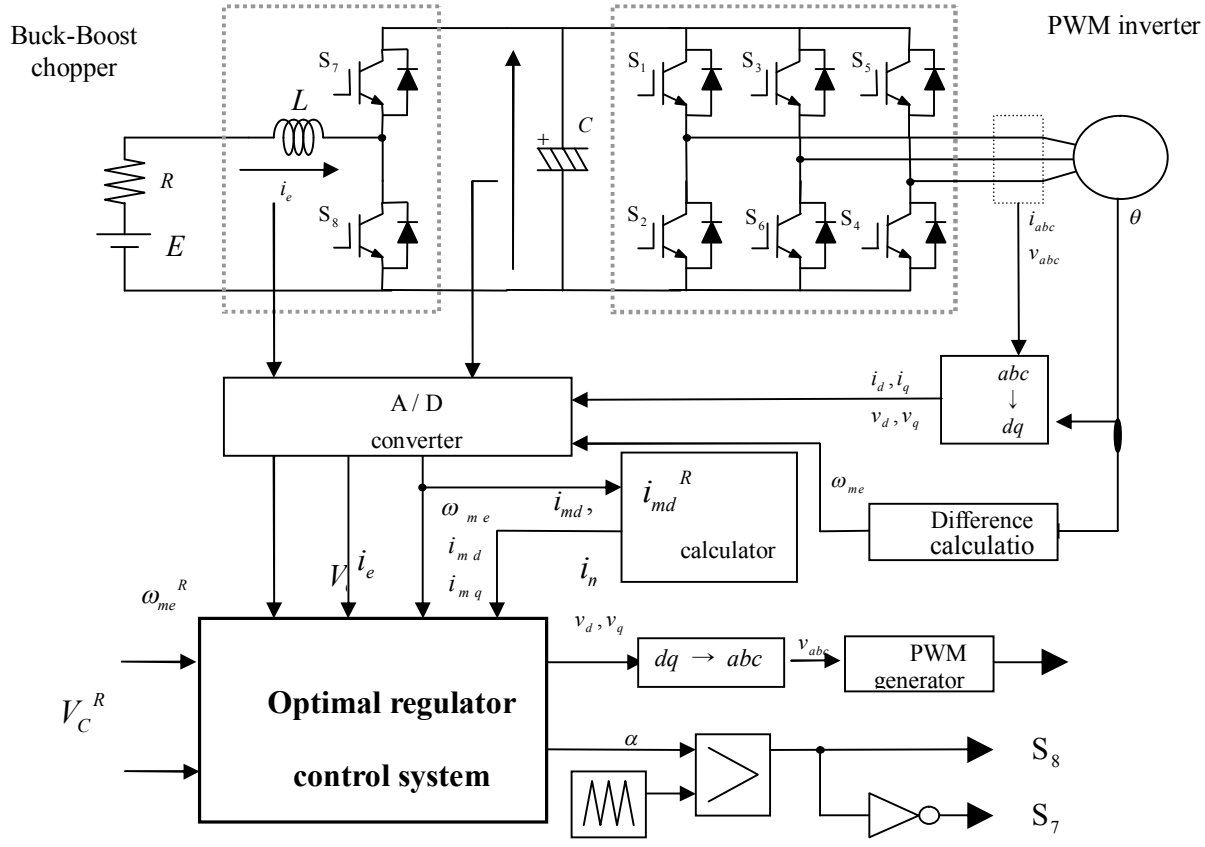

Fig. 5. System configuration by optimal regulator

$$\mathbf{PI}=\sum_{i=1}^{\infty}\{\mathbf{X}_0^{\mathrm{T}}(k)\mathbf{Q}\mathbf{X}_0(\mathrm{k})+\Delta\mathbf{u}^{\mathrm{T}}(k)\mathbf{H}\Delta\mathbf{u}(k)\} \quad (30)$$

$$\Delta\mathbf{u}(k)=-\left[\mathbf{H}+\mathbf{G}^{T}\mathbf{P}\mathbf{G}\right]^{-1}\mathbf{G}^{T}\mathbf{P}\Psi\mathbf{X}_0(k)=\mathbf{F}_{\mathrm{B}}\mathbf{X}_0(k) \quad (31)$$

$$\mathbf{F_B}=-\left[\mathbf{H}+\mathbf{G}^{\mathrm{T}}\mathbf{P}\mathbf{G}\right]^{-1}\mathbf{G}^{\mathrm{T}}\mathbf{P}\Psi \quad (32)$$

It is known that the matrix **P** converges to the constant matrix at steady state.

The basic control system structure applied on the optimal regulator is shown in Fig.4. The optimal regulator system based on the error system guarantees that the error between the output and the desired value converges to zero . The switching of the PWM inverter is carried out every sampling period according to the subsequent control input in eq.(31) [6].

Table 1. Constants of testing machine

Rated power	475 .0[W]
Rated rotor speed	1800.0[min^{-1}]
Rated torque	2.52 [Nm]
Number of pole pair	2.0
Magnetic flux linkage	0.1 [Wb]
Stator resistance	0.5 [Ω]
Core loss resistance	300.0 [Ω]
d-axis inductance	0.009 [H]
q-axis inductance	0.0228 [H]
Inertia(only motor)	0.00255 [kg-m^2]

5. Simulation Results

In order to confirm the validity of the proposed model, some simulations are carried out utilizing MATLAB and the laboratory machine. The testing machine constants are shown in Table 1. In order to simulate the reduced model, the inertia *J* of the reduced IPMSM drive system is referred to the real hybrid vehicle, considering the car weight. This is done by assuming that the energy of $(1/2)J\omega^2$ equals $(1/2)mv^2$, where *m* is the car weight and *v* is the velocity of

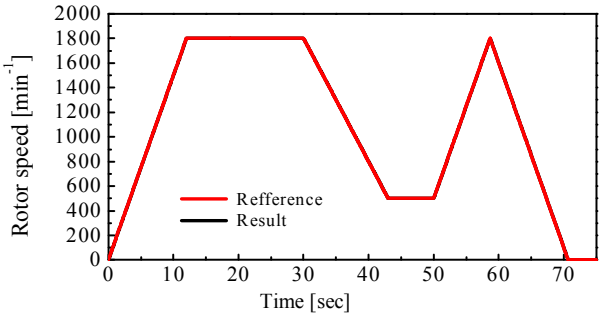

(a) Rotor speed

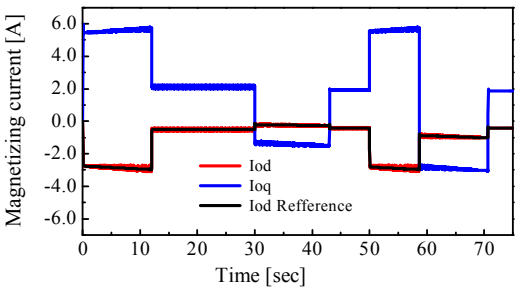

(b) Magnetizing current

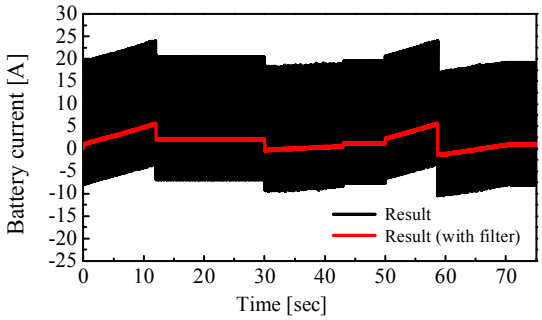

(c) Battery current

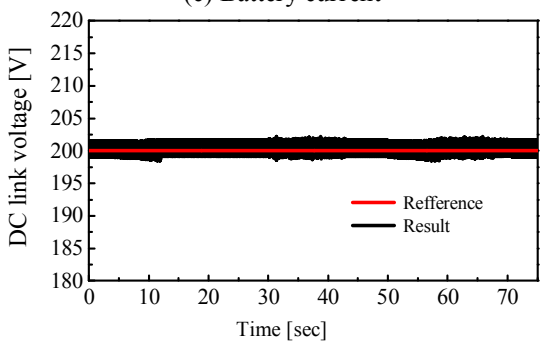

(d) DC link voltage

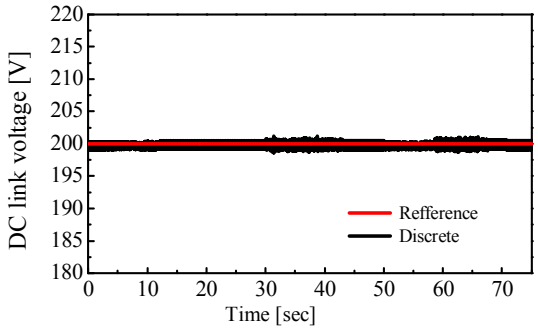

(e) Discrete DC link voltage

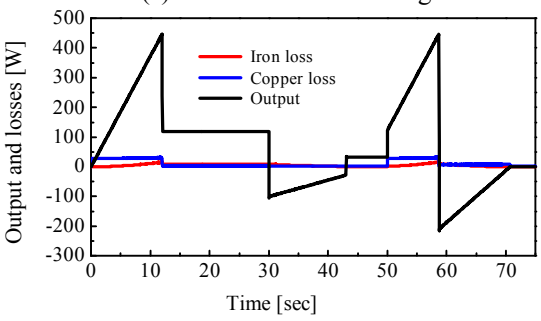

(f) Output and losses

Fig. 6. Simulation results

the car. The car weight of the testing drive system is 14.25 kg and the moment of inertia J is 0.117 kg-m^2, so that the car weight of the Prius class is about 1500 kg and the maximum motor output is 50 kW.

The control system configuration used in the simulation is shown in Fig.5. The quadrant chopper is also controlled by the optimal regulator. In order to utilize techniques such as MATLAB or the look-up table method [6], it is necessary to prepare the feedback gain file shown in eqs. (31) and (32) in advance. The system consists of the PWM inverter and the two-quadrant chopper (used to switch the buck chopper and boost chopper), which can control the DC link voltage from the battery to store regenerative energy temporarily. In this model, the output of the IPMSM is restricted to a maximum of 20 kW.

Fig.6 shows simulation results using the reduced model. Fig.6(a) shows the response to variable speed, considering fuel mode under the assumption of the application of the hybrid vehicle. Fig.6(b) shows responses for the desired magnetizing currents for Maximum Torque/Ampere control. The d-axis magnetizing current is controlled to the desired value satisfying the Maximum Torque/Ampere control algorithm. Fig.6(c) shows responses for the battery current. The section below the zero line signifies the regeneration of power to the supply. The DC link voltage is controlled to be 200 V, as shown in Fig.6(e). Fig.6(f) shows the output power, copper loss and iron loss. The iron loss rises according to the output power increase, and the copper loss varies by step change under acceleration.

6. Conclusions

In this paper, the IPMSM drive system for hybrid vehicles is modeled from a view point of the state space method. Various control techniques, such as speed control, maximum efficiency operation, and Maximum Torque/Ampere control, are realized by applying the multi-input and multi-output optimal regulator theories simultaneously. Regarding simulation results, it can be concluded that good speed response with Maximum Torque/Ampere control is achieved , and the desired DC voltage with unity power factor is also achieved by using the proposed optimal regulator control system. Further research for designing a controller that includes the IPMSM design is required. The modeling and simulation techniques in our paper are powerful design methods that can be used.

Appendix : State equations of the IPMSM

An equivalent circuit of the IPMSM taking core losses into account is shown in Fig.7. Basic equations are obtained from the equivalent circuit considering core loss resistance as follows.

$$\mathbf{v_a} = R_a\mathbf{i_a} + R_m\mathbf{i_c} \tag{A-1}$$

$$R_m\mathbf{i_c} = \frac{d\boldsymbol{\lambda}}{dt} + j\omega_{me}\boldsymbol{\lambda} \tag{A-2}$$

$$\mathbf{i}_a = \mathbf{i}_c + \mathbf{i}_m \tag{A-3}$$

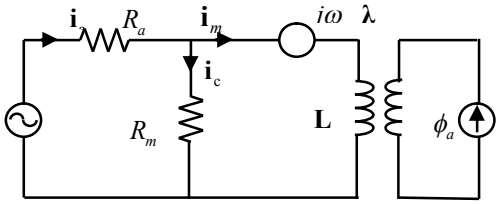

Fig. 7. Equivalent circuit of IPMSM

where variables for voltage, flux linkage and current mean vector are defined as follows [7].

$$\mathbf{v_a} = v_d + jv_q, \boldsymbol{\lambda} = \lambda_d + j\lambda_q, \mathbf{i_a} = i_d + ji_q$$

The flux linkage equations of the d-q axes with rotating reference frame and fixed rotor are as follows.

$$\lambda_d = L_d i_{md} + \phi_a, \quad \lambda_q = L_q i_{mq} \tag{A-4}$$

Then the electromagnetic torque is expressed by the following equation:

$$T_e = p\left(\lambda_d i_{mq} - \lambda_q i_{md}\right) = p\left\{\left(L_d - L_q\right) i_{md} i_{mq} + \phi_a i_{mq}\right\} \tag{A-5}$$

where p denotes the pole pair number.

From eq. (A-1)~(A-3), the state equations of the IPMSM, considering core losses, are then:

$$\frac{di_{md}}{dt} = \omega_{me} i_{mq} \frac{L_q}{L_d} - \left(\frac{R_m}{R_a + R_m}\right)\frac{R_a}{L_d} i_{md} + \left(\frac{R_m}{R_a + R_m}\right)\frac{v_d}{L_d} \tag{8}$$

$$\frac{di_{mq}}{dt} = -\frac{\omega_{me}}{L_q}\left(L_d i_{md} + \phi_a\right) - \left(\frac{R_m}{R_a + R_m}\right)\frac{R_a}{L_q} i_{mq} \tag{9}$$

References

[1] K. Yamamoto, K. Shinohara and S. Furukawa, "Permanent Magnet Synchronous Motor Driven by PWM Inverter with Voltage Booster with Regenerating Capability Augmented by Double-Layer Capacitor", *IEEJ Trans IA*, Vol. 126, No. 5, pp. 639-645 (2006).

[2] J.C. Liao and S.N. Yeh, "A Novel Instantaneous Power Control Strategy and Analytical Model for Integrated Rectifier/Inverter Systems", *IEEE Trans. Power Electronics*, Vol. 15, No. 6, pp. 996-1006 (2000).

[3] T.G. Habetler, "A Space Vector-Based Rectifier Regulator for AC/DC/AC Converters", *IEEE Trans. Power Electronics*, Vol. 8, No. 1, pp. 30-36 (1993).

[4] Atsuo Kawamura, *Modern Power Electronics*, Saiensu Co Ltd. (2002) (in Japanese).
[5] M. Takiguchi, T. Murata, J. Tamura, T. Tsuchiya, "Maximum Torque/Minimum Flux Control of Interior Permanent Magnet Synchronous Motor Based on Magnetic Energy Model", *12th European Conference on Power Electronics and Applications (EPE2007)*, No. 0625, (10 pages), 2007/9.
[6] T. Murata, H. Taka, J. Tamura, T. Tsuchiya, "Field Oriented Control of Brushless DC Motor Driven by Control Algorithm Applied on Modern Control Theory", *Conference Record of ICEM 2002 (International Conference on Electrical Machines)*, No. 593, (5 pages), 2002/8.
[7] P.K. Kovac, *Transient Phenomena in Electrical Machines*, Chap.1, Elsevier (1984).
[8] B. Adkins and R.G. Harley, *General Theory of Alternating Current Machines*, Chap.6, p.124, Chapman and Hall (1975).

Toshiaki Murata received Dr. Eng. from Hokkaido University in 1992. His research interests are motor control, especially field oriented control. He retired from Kitami Institute of Technology in 2010 as Associate Professor of the Department of Electric and Electrical Engineering.

Utaro Kawatsu received B.S. degree in Communication Engineering from Tohoku University in 2011. He works for The Aisin AW Co., Ltd.

Junji Tamura received his Dr. Eng. from Hokkaido University in 1984. He is professor in Kitami Institute of Technology. He is now a vice-president for education. He is a member of the IEE of Japan and a senior member of the IEEE Power Engineering Society.

Takeshi Tsuchiya obtained his Dr. Eng. from Hokkaido University in 1974. Upon graduation, he has been a professor of Hokkaido University. He is a member of the Institute of Electrical Engineering of Japan, the Society of Instrument and Control Engineers(Japan), and the Japan Association of Automatic Control Engineers, and a fellow of the IEEE.